HAL
open science

Plasma clouds and snowplows: Bulk plasma escape from Mars observed by MAVEN

J. S. Halekas, D. A. Brain, S. Ruhunusiri, J. P. Mcfadden, D. L. Mitchell, C. Mazelle, J. E. P. Connerney, Y. Harada, T. Hara, J. R. Espley, et al.

To cite this version:

J. S. Halekas, D. A. Brain, S. Ruhunusiri, J. P. Mcfadden, D. L. Mitchell, et al.. Plasma clouds and snowplows: Bulk plasma escape from Mars observed by MAVEN. Geophysical Research Letters, 2016, 43, pp.1426-1434. 10.1002/2016GL067752 . insu-03675431

HAL Id: insu-03675431

https://insu.hal.science/insu-03675431

Submitted on 23 May 2022

HAL is a multi-disciplinary open access archive for the deposit and dissemination of scientific research documents, whether they are published or not. The documents may come from teaching and research institutions in France or abroad, or from public or private research centers.

L'archive ouverte pluridisciplinaire **HAL**, est destinée au dépôt et à la diffusion de documents scientifiques de niveau recherche, publiés ou non, émanant des établissements d'enseignement et de recherche français ou étrangers, des laboratoires publics ou privés.

Copyright

AGU PUBLICATIONS

Geophysical Research Letters

RESEARCH LETTER
10.1002/2016GL067752

Key Points:
- Ionospheric plasma can escape from Mars in coherent structures or clouds
- Momentum is transferred from the solar wind to heavy ions by magnetic fields
- A snowplow effect accelerates parcels of unmagnetized Martian plasma

Correspondence to:
J. S. Halekas,
jasper-halekas@uiowa.edu

Citation:
Halekas, J. S., et al. (2016), Plasma clouds and snowplows: Bulk plasma escape from Mars observed by MAVEN, *Geophys. Res. Lett.*, *43*, 1426–1434, doi:10.1002/2016GL067752.

Received 11 JAN 2016
Accepted 7 FEB 2016
Accepted article online 10 FEB 2016
Published online 25 FEB 2016
Corrected 10 MAR 2016

This article was corrected on 10 MAR 2016. See the end of the full text for details.

©2016. American Geophysical Union. All Rights Reserved.

Plasma clouds and snowplows: Bulk plasma escape from Mars observed by MAVEN

J. S. Halekas[1], D. A. Brain[2], S. Ruhunusiri[1], J. P. McFadden[3], D. L. Mitchell[3], C. Mazelle[4], J. E. P. Connerney[5], Y. Harada[3], T. Hara[3], J. R. Espley[5], G.A. DiBraccio[5], and B. M. Jakosky[2]

[1]Department of Physics and Astronomy, University of Iowa, Iowa City, Iowa, USA, [2]Laboratory for Atmospheric and Space Physics, University of Colorado Boulder, Boulder, Colorado, USA, [3]Space Sciences Laboratory, University of California, Berkeley, California, USA, [4]L'Institut de Recherche en Astrophysique et Planétologie, Toulouse, France, [5]NASA Goddard Space Flight Center, Greenbelt, Maryland, USA

Abstract We present initial Mars Atmosphere and Volatile EvolutioN (MAVEN) observations and preliminary interpretation of bulk plasma loss from Mars. MAVEN particle and field measurements show that planetary heavy ions derived from the Martian atmosphere can escape in the form of discrete coherent structures or "clouds." The ions in these clouds are unmagnetized or weakly magnetized, have velocities well above the escape speed, and lie directly downstream from magnetic field amplifications, suggesting a "snowplow" effect. This postulated escape process, similar to that successfully used to explain the dynamics of active gas releases in the solar wind and terrestrial magnetosheath, relies on momentum transfer from the shocked solar wind protons to the planetary heavy ions, with the electrons and magnetic field acting as intermediaries. Fluxes of planetary ions on the order of 10^7 cm^{-2} s^{-1} can escape by this process, and if it operates regularly, it could contribute 10–20% of the current ion escape from Mars.

1. Introduction and Context

Though superficially similar to the Earth's magnetosphere, the Martian magnetosphere operates in a fundamentally different manner, with planetary plasma forming the primary obstacle to the solar wind [*Nagy et al.*, 2004]. As a result, the structure of the magnetosphere differ from the terrestrial case, with the magnetopause replaced by an induced magnetospheric boundary (IMB) that forms the interface between plasma of solar wind and planetary origin, as shown by Phobos 2 and Mars Express [*Lundin et al.*, 1990; *Rosenbauer et al.*, 1989; *Sauer et al.*, 1994; *Dubinin et al.*, 2008]. The Martian magnetosphere fundamentally depends on mass loading [*Szego et al.*, 2000] in a manner unlike the Earth, and in many ways more like comets. Despite these contrasts, many plasma processes with terrestrial analogues operate at Mars, including the formation of a magnetotail and plasma sheet [*Fedorov et al.*, 2006; *Harada et al.*, 2015; *DiBraccio et al.*, 2015], reconnection [*Eastwood et al.*, 2008; *Dubinin et al.*, 2008] and flux rope generation [*Brain et al.*, 2010; *Hara et al.*, 2015], and low-frequency fluctuations [*Espley et al.*, 2004; *Winningham et al.*, 2006], some of which may arise from shear-driven instabilities [*Penz et al.*, 2004; *Gunell et al.*, 2008; *Gurnett et al.*, 2010]. These diverse processes can all facilitate the escape of planetary ions from Mars [*Dubinin et al.*, 2011].

The Mars Atmosphere and Volatile EvolutioN (MAVEN) mission, designed to understand the escape of atmospheric gases from Mars [*Jakosky et al.*, 2015], arrived at Mars in September 2014. Since then, MAVEN has made progress on characterizing the net escape rate of ions with energies $>$ 25 eV [*Brain et al.*, 2015]. A significant fraction of this escape takes place through a pickup ion "plume"; however, a larger fraction escapes down the tail and around the flanks [*Dong et al.*, 2015]. Though MAVEN has measured the total rate, it has not yet evaluated all the escape channels, and it has not characterized the lowest-energy component of the ion escape.

Bulk plasma loss—or escape of planetary plasma in the form of coherent structures—constitutes one escape channel postulated to occur at Mars, based primarily on the analogy to Venus, where Pioneer Venus Orbiter observed detached plasma clouds, seemingly separated from the main ionosphere [*Brace et al.*, 1982; *Russell et al.*, 1982]. Observations showing large-amplitude structures in and near the ionosphere [*Gurnett et al.*, 2010; *Halekas et al.*, 2011] and apparently detached features in ionospheric density profiles [*Dubinin et al.*, 2011] suggest that such bulk plasma escape processes also occur at Mars. In this paper, we present the first preliminary observations and interpretation of bulk plasma loss at Mars from MAVEN.

2. Bulk Plasma Loss Observed by MAVEN

MAVEN's comprehensive plasma instrumentation and its inclined elliptical orbit, which precesses rapidly and samples different portions of the Martian environment, make it ideal for observing ion escape processes throughout the magnetosphere [*Jakosky et al*., 2015]. In July 2015 MAVEN's orbit lay near the dawn-dusk plane, allowing it to cut across the IMB at the flank, perpendicular to the solar wind flow. We present magnetic field and charged particle observations from Magnetometer [*Connerney et al*., 2015], Solar Wind Electron Analyzer (SWEA), Solar Wind Ion Analyzer [*Halekas et al*., 2013], and Suprathermal and Thermal Ion Composition (STATIC) [*McFadden et al*., 2014] during the inbound portion of one such orbit in Figure 1, which shows an interval containing the transition from the magnetosheath into the ionosphere. In the sheath, the magnetic field pointed in the $-X/+Y/+Z$ direction, consistent with the draping pattern expected for an interplanetary magnetic field (IMF) orientation in the $+Y/+Z$ quadrant in Mars Solar Orbital (MSO) coordinates. Given this IMF direction and antisunward ($-X$) flow, MAVEN's location in the $+Y/-Z$ quadrant places it in the hemisphere where the motional electric field $\boldsymbol{E_c} = -\boldsymbol{v} \times \boldsymbol{B}$ points into the magnetosphere (the $-Z$ hemisphere in Mars Solar Electric (MSE) coordinates). A pickup ion plume on the outbound side of the orbit (not shown) supports this inference for the location of the observation. During the interval in Figure 1, B_x reverses, indicating that MAVEN crosses the induced current sheet (the MSE X-Z plane). Straddling this reversal, we observe several coherent structures in the magnetic field, and during the same time interval we find sheath protons interspersed with discrete bunches of heavy ions, and several sharp enhancements in electron flux.

It is highly tempting to interpret these structures as flux ropes or plasmoids containing escaping planetary plasma, as previously reported by Mars Global Surveyor (MGS) and MAVEN [e.g., *Eastwood et al*., 2008; *Brain et al*., 2010; *Hara et al*., 2015]. However, though the magnetic field does show evidence of some twisting, the time sequence of events in Figure 1 strongly disfavors this interpretation. The enhancements in planetary plasma density precede the magnetic field structures (dashed vertical lines on the figure mark their leading edge), and, in fact, we only observe small fluxes of planetary ions at the times of peak magnetic field amplification. Furthermore, though they have some bipolar components, the magnetic structures do not have the polarization signature expected for a force-free flux rope.

The directed and thermal pressures of the ions help clarify their nature. In the sheath, the shocked solar wind protons have much higher directed (dynamic) pressure, consistent with the supersonic flow typically seen in the flank magnetosheath. The interspersed heavy ion populations consist of nearly even admixtures of atomic and molecular oxygen ions, with comparable directed and thermal pressures, and energies from a few eV to a few hundred eV. The two species have approximately equal energies, suggesting acceleration through an electrostatic potential. Finally, a distinct high-energy ~10 keV O^+ population originates from pickup in the distant corona [*Dong et al*., 2015].

In steady state, the momentum flux, which we can write for an isotropic plasma in the form $\rho \vec{U}\left(\vec{U}\cdot\hat{n}\right) + p\hat{n} - \left[\frac{\vec{B}\left(\vec{B}\cdot\hat{n}\right)}{\mu_0} - \frac{B^2}{2\mu_0}\hat{n}\right]$ (ρ, p, U, and B represent mass density, thermal pressure, flow velocity, and magnetic field), should be continuous across any boundary. We plot the dynamic, thermal, and normal magnetic pressure components in Figure 1. For the boundary normal $\hat{n}$, we use a value of [–0.94,–0.35, 0.02], estimated by performing minimum variance across the first discontinuity at 14:55 UT (the result does not change significantly for any normal direction pointing primarily along $\pm X$). Intriguingly, the electron and normal magnetic pressure so derived both maximize at the interfaces between the sheath protons and the planetary ions, with the total rising almost up to the total heavy ion pressure at the other side of the interface (if we could account for curvature forces, they might balance more closely) suggesting a mechanism whereby the momentum of the sheath protons is transferred to the heavy ions using the electrons and/or magnetic fields as intermediaries. We will discuss this scenario further below. The total momentum flux changes with time, implying an episodic rather than steady state process. Consistent with this inference, the heavy ion populations evolve within each discrete event and also along the orbit. Closer to the planet, we observe a repeating pattern, with a dispersion feature (higher energies, then lower), and then a high flux population directly preceding each magnetic amplification. Farther from the planet, we find higher ion energies, implying greater acceleration.

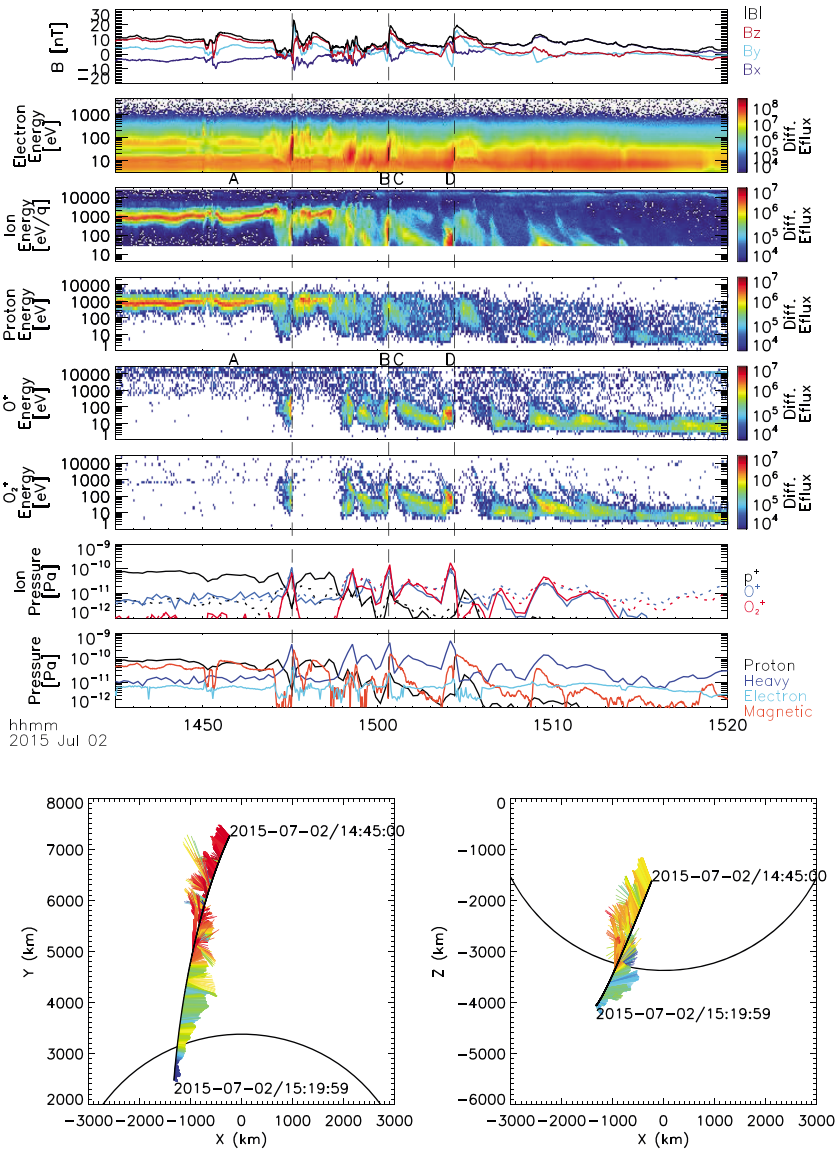

Figure 1. MAVEN observations along an inbound orbit segment, transitioning from the Martian magnetosheath to the magnetosphere. The eight time series panels show magnetic field components, electron energy spectra, total ion spectra, proton, O^+, and O_2^+ spectra, ion thermal (dashed) and dynamic (solid) pressure components, and the total pressures associated with protons, heavy ions, electrons, and the transverse magnetic field. All energy spectra have units of eV/(eV cm^2 s sr). In calculating electron pressures, we corrected for the effects of spacecraft potential and photoelectrons (visible at energies below ~10 eV at times with sheath plasma present). The magnetic field pressure includes the normal component but not the tension component due to curvature. The two panels at the bottom show projections of the orbit, with the magnetic field in-plane direction and magnitude indicated by individual whiskers, and the out-of-plane component indicated by color (red = out of plane, green = in plane, and blue = into plane). A, B, C, and D indicate the times when MAVEN measured the distribution functions shown in Figure 2. Vertical dashed lines mark the current sheet at the leading edge of the magnetic field amplifications. All vector quantities utilize Mars Solar Orbital (MSO) coordinates.

Figure 2 shows charged particle distributions from STATIC and SWEA. In the sheath, at time "A," the protons have a tailward and outward directed ($-X/+Y$) flow on the order of 300 km/s, consistent with the expected deflected flow of shocked protons of solar wind origin. The electrons observed at the same time have a high temperature, with higher parallel than perpendicular components, typical for the flank magnetosheath.

At the leading edge of one of the magnetic amplifications, at time "B," the main proton component remains but diminished in flux (note different color scales), implying that some protons have been reflected or deflected

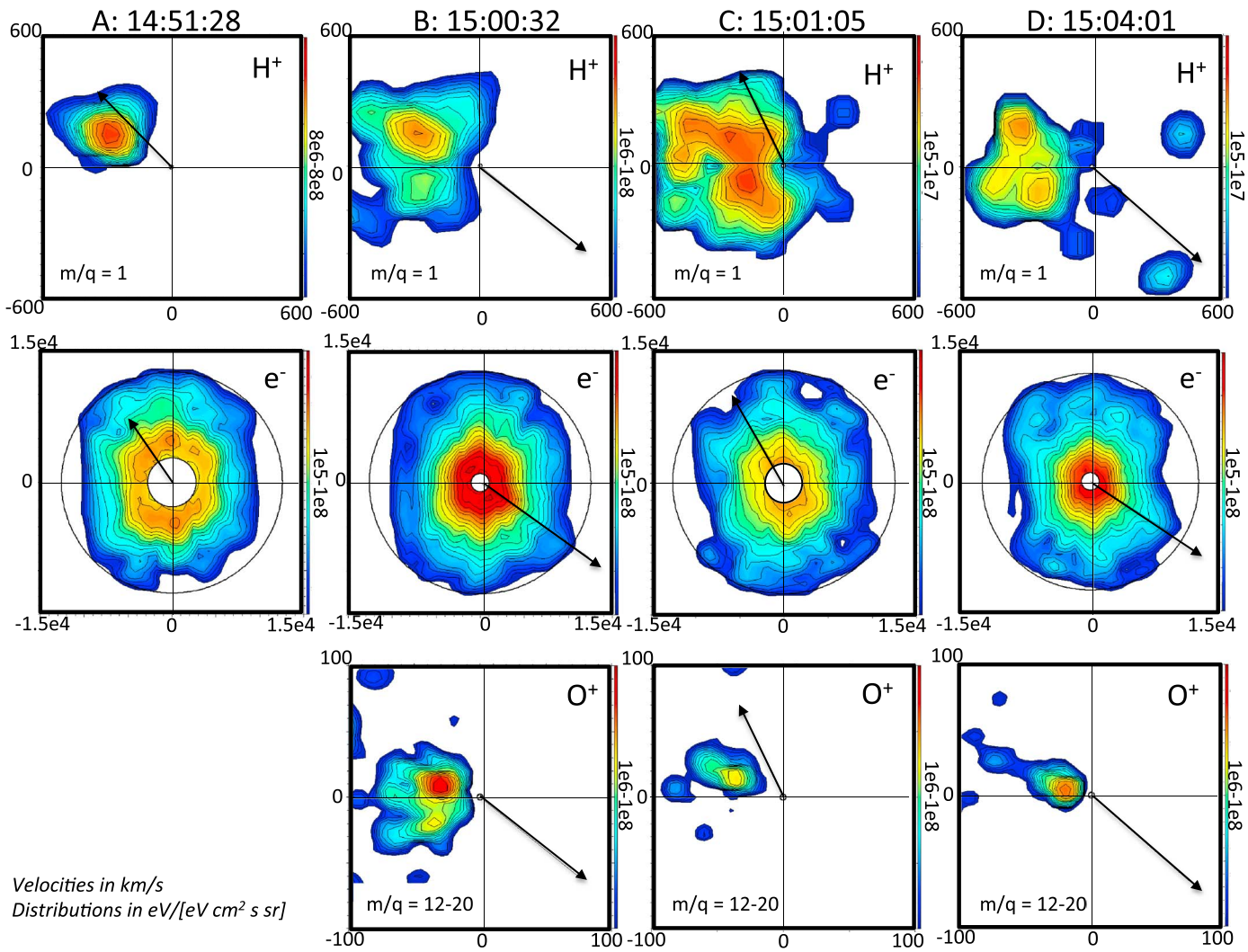

Figure 2. Cuts through 3-D velocity distributions in the *X-Y* MSO plane for protons, electrons, and atomic oxygen ions at times A, B, C, and D (we omit an O^+ distribution at time A due to the lack of any appreciable flux at the velocities shown). The lowest energy for electrons is chosen to exclude spacecraft photoelectrons. Arrows in each panel show the projection of the measured magnetic field to this plane. Note the different color scales for each H^+ distribution.

around the structure, and a separate proton component with an inward velocity in the $-X/-Y$ direction appears, traveling roughly perpendicular to the magnetic field. This second population could consist of solar wind or planetary hydrogen. The electrons have a higher density (indicating compression) but lower temperature, possibly indicating a component of ionospheric photoelectrons, and retain some anisotropy. The oxygen ions have a directed flow of ~30 km/s in roughly the same direction as the original sheath protons, together with a second component with comparable flow speed and a flow direction similar to the second proton component.

Just after the magnetic amplification, at time "C," the proton distribution shows a further reduction in flux (note different color scales), with multiple overlapping components similar to those at time B, but with a less distinct separation. The electrons have a higher temperature and lower density, and some indication of an anti-field-aligned component. The oxygen ions have only a single low-energy component, with a direction similar to that of the original sheath protons. Intriguingly, this feature shows some indication of broadening along the flow direction, suggesting a range of O^+ ions with the same flow direction, but different flow speeds.

At time "D," at the leading edge of the next magnetic amplification, the proton flux diminishes still further, with similar velocity components to the previous two times. The electrons have a lower temperature, show evidence of compression, and have a large field-aligned component. The oxygen ions at this time have an even greater spread in velocities, all flowing in the same direction as the original sheath flow but with a wide range in flow speed.

We note that the large differences in flow speed between the sheath plasma and the heavy ions appear inconsistent with mature Kelvin-Helmholtz vortices [*Penz et al*., 2004] (which should accelerate some ionospheric plasma up to speeds comparable to the sheath flow). However, shear instabilities could play a role in developing the initial structuring of the topside ionosphere that likely precedes the formation of the structures we describe here and may be responsible for the twisting of the magnetic field that we see in some of the structures. The flow speed of the heavy ions (much greater than escape velocity) strongly suggests that these structures will escape the planet, though it does not prove their detachment. It also indicates that unless the structures themselves stand in the flow while their constituents move downstream (unlikely given the widely varying ion velocities), MAVEN encounters these structures as they convect over the spacecraft. This suggests that the heavy ion dispersion signatures that precede the peaks in heavy ion flux, which in turn directly precede the compressed electrons and magnetic amplifications, may represent at least in part the spatial evolution of a structure (with the spacecraft effectively moving from the downstream to upstream side as the structure convects over it) rather than solely temporal variability or lateral inhomogeneity.

To understand the observations presented in the preceding section, we need to consider how the magnetized sheath flow will interact with an obstacle consisting of unmagnetized or weakly magnetized ionospheric plasma. A likely interpretation stems from the lithium and barium releases performed by the Active Magnetospheric Particle Tracer Explorers (AMPTE) in the solar wind and magnetosheath, which produced a physical scenario in many ways similar to that encountered here and to that seen in ionospheric plasma clouds at Venus.

3. Snowplow Mechanism for Bulk Plasma Acceleration

The AMPTE releases of unmagnetized material resulted in the formation of an initial diamagnetic cavity, which external plasma and fields could not penetrate [*Gurnett et al*., 1985]. Upstream from this cavity, the magnetic field became compressed, with a narrow region of overlap between compressed magnetic field and heavy ions [*Gurnett et al*., 1985]. As elucidated by *Haerendel et al*. [1986], at a microscopic level, this resulted from the differential motion of electrons (magnetized) and ions (unmagnetized) at the boundary of the heavy ion plasma, which produced a polarization electric field and resulted in a shielding current driven by the drifts of the electrons. This shielding current canceled out the magnetic field in the cavity and produced the amplified fields upstream.

Figure 3 shows a proposed scenario for how such a process might operate at Mars. Given an unmagnetized or weakly magnetized ionosphere, if inhomogeneities initially form in the topside ionosphere or at the IMB (possibly due to shear instabilities), and if the planetary ions have energies $\geq$1 eV (quite commonly observed at higher altitudes), such incipient structures can easily have scale sizes not dramatically larger than the gyroradii of the planetary ions in the sheath field ($\geq$100 km). In this case, initially unmagnetized heavy ions will try to propagate freely outward into the sheath. However, electrons will remain strongly magnetized, gyrating around the field at the boundary between sheath and planetary plasma. This will produce a polarization electric field E_P to maintain quasi-neutrality, leading to the formation of a shielding current J_S. This current will keep the magnetic field in the planetary plasma weak and steepen and compress it at the upstream boundary to form a so-called "snowplow," leading to draping of the sheath magnetic field around the planetary plasma [*Haerendel et al*., 1986]. As described by *Szego et al*. [2000], in the upstream region the magnetic normal pressure and tension forces should balance, but downstream they will add to produce a downstream directed force on the planetary plasma. Note that this implies that the magnetic pressure shown in Figure 1 constitutes a lower limit to the magnetic forces on the planetary ions, with the tension forces more important for smaller lateral scale sizes.

The cartoon in Figure 3 describes the hypothesized initial stages of the interaction between the magnetized sheath plasma and the planetary plasma. At later stages, the snowplow would propagate through the heavy ions, accelerating them downstream. *Haerendel et al*. [1986] gives a first-order expression for the snowplow speed of $v_{sp} \sim 2B_{max}/\sqrt{\mu_0 \rho_{heavy}}$, which for the MAVEN observations works out to ~20–40 km/s, comparable to the speed of the heavy ions we observe in the discrete bunches of heavy ions, but much slower than the sheath proton flow speed of ~350 km/s.

In addition to the portion of the planetary plasma gradually accelerated by the snowplow, electric fields at the boundaries of the unmagnetized plasma will extract ions that can reach even higher velocities [*Haerendel et al*., 1986; *Chapman*, 1989a, 1989b; *Chapman and Schwartz*, 1987]. The motional electric field

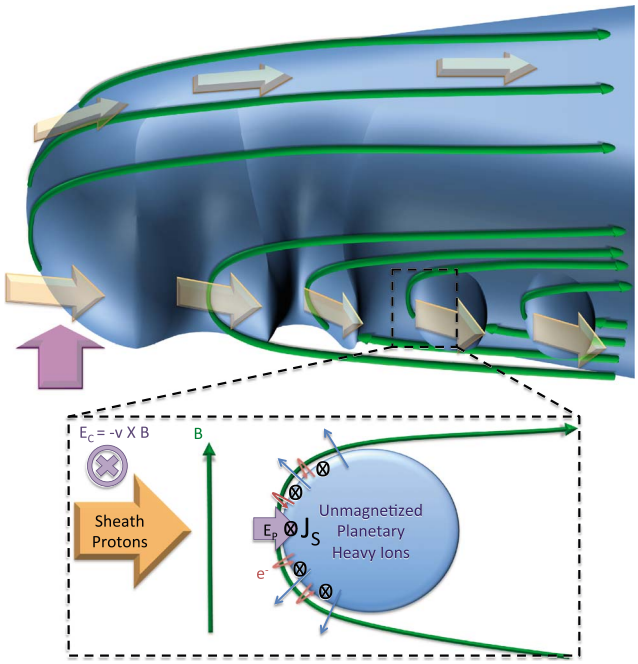

Figure 3. Schematic illustration of a possible interpretation of MAVEN observations, showing a "wavy" induced magnetosphere boundary with rays of ionospheric plasma and/or detached plasma clouds interspersed with sheath plasma of solar wind origin. Inset shows the expected polarization electric field E_P and the associated shielding currents J_S that form the snowplow, caused by the differential motion of ionospheric electrons and heavy ions at the boundary between magnetized sheath and unmagnetized ionospheric plasma.

E_C of the sheath plasma will accelerate ions inward (into the magnetosphere) from the leading and inner edge of the structure, and the polarization electric field E_P at the leading edge will accelerate ions downstream that will pass through the structure at higher velocities. These extracted ions necessarily transfer momentum from the structure.

If our interpretation proves correct, the MAVEN observations represent a detached cloud passing over the spacecraft as it accelerates downstream under the influence of the snowplow effect described above. The energy dispersion we observe may result from time dispersion of extracted ions accelerated in regions of the structure with different electric field strengths and/or may reflect acceleration in electric fields that vary temporally as the structure evolves and accelerates downstream. The range of heavy ions with similar flow directions but different flow speeds seen at times C and D also appears consistent with acceleration in a spatially and/or temporally variable electric field pointing in the direction of the snowplow motion (roughly the same as the sheath flow direction). Lending yet more credence to the scenario, we observe a second component of both hydrogen and oxygen ions accelerated inward, perpendicular to the magnetic field, potentially representing ions from the leading edge of the structure (as well as newly ionized planetary ions) accelerated in the direction of the sheath motional electric field E_C.

4. Global Context for Bulk Plasma Loss From Mars

Observations of the sort presented in Figures 1 and 2 have proven relatively common during MAVEN's first year in orbit. While we have not yet performed a full statistical study of their occurrence, we estimate that similar features occur on ~5–10% of MAVEN orbits. This occurrence rate represents a convolution of the chance of observing the structures and the chance of their formation. Some reasons exist to think that they may occur quite frequently but that MAVEN must pass through the right region of the magnetosphere to see them.

We show a second example set of observations, in the same format, in Figure 4. During this time period, MAVEN's periapsis lay on the dayside, allowing it to sample the flank and tail. In contrast to the case in Figure 1, MAVEN traveled outbound on this orbit segment, from the tail to the sheath. Just as in that case, the inferred IMF direction (primarily $+Y$ MSO) indicates a location in the $-Z$ MSE hemisphere. All such observations that we have examined in detail share this feature, suggesting that these features preferentially occur in the $-Z$ MSE hemisphere, implying that we require favorable IMF geometry to observe them. This location bias may arise as a result of the effects of the recoil forces on the planetary plasma (required by conservation of momentum to balance ion extraction) [*Haerendel et al.*, 1986], which will accelerate the cloud in the direction opposite the motional electric field E_C in the sheath (and thus outward in the $-Z$ MSE hemisphere), favoring the detachment and escape of plasma clouds in this hemisphere.

Despite the different orbital geometry for this time period, we observe structures with the same character as those presented above, consisting of dispersed heavy ion populations immediately preceding magnetic

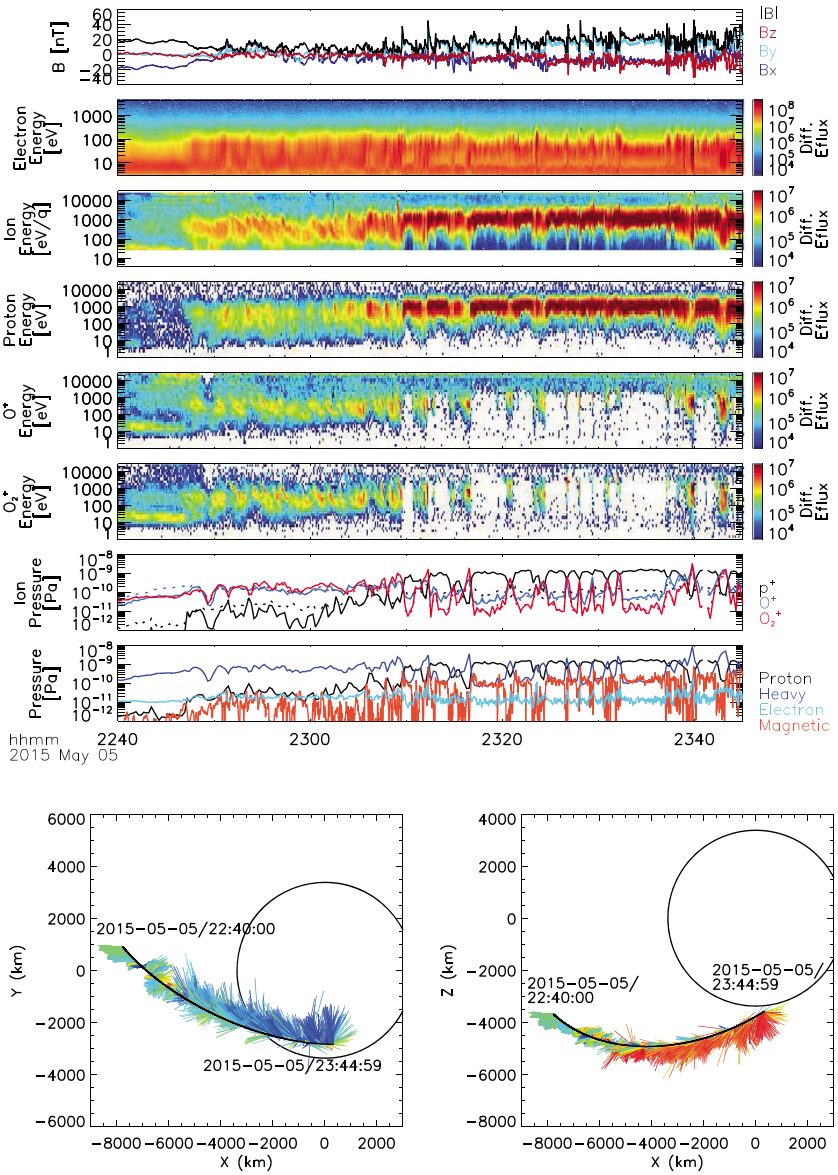

Figure 4. MAVEN observations similar to those shown in Figure 1, in the same format, for a different orbital geometry, along an outbound orbit segment.

amplifications, interspersed among sheath plasma. The energy of the escaping heavy ions evolves in a similar way, with lower maximum energies closer to the tail, and higher energies as we travel outward into the sheath. The consistent temporal ordering of the features, despite the opposite direction of spacecraft motion, strongly supports the hypothesis that these represent structures convecting over the spacecraft and provides further support for the idea that they form detached clouds of escaping plasma.

We note a clear evolution of the dispersion features, with greater dispersion seen closer to the central tail. These signatures may represent ions extracted from the snowplow as it evolves, which then disperse in energy as they travel inward toward the center of the tail. Therefore, the bulk loss process discussed in this paper may provide a source for the variable electric fields postulated to explain commonly observed time-dispersed ion signatures, which also occur preferentially in the $-Z$ MSE hemisphere [*Halekas et al.*, 2015]. This process may also be related to the "sawtooth" events previously observed by MGS, which consist of quasiperiodic magnetic amplifications near the topside of the ionosphere [*Halekas et al.*, 2011]. Finally, we conjecture that this process could help explain the tail "loading/unloading" described by *DiBraccio et al.* [2015], which may represent the periodic release of draped field lines as they pull parcels of planetary plasma downstream.

5. Conclusions and Implications

We have presented the first observations and a potential interpretation of bulk plasma loss from Mars observed by MAVEN. Our observations support the idea that ionospheric plasma can be lost from Mars in the form of coherent structures—"clouds"—accelerated by a snowplow effect. The postulated escape process depends on momentum transfer from the shocked solar wind protons to the planetary heavy ions, with the electrons and magnetic field acting as intermediaries.

Work remains to be done to place these observations in a global context, determine their coupling to other magnetospheric processes, and to further investigate the microphysics of the interaction, particularly the electron kinetics and the currents and electric fields at the snowplow boundary and the downstream edge of the plasma cloud. In addition, we need to determine the global significance of this escape process. The observations presented in this manuscript reveal fluxes on the order of $10^7\,\mathrm{cm}^{-2}\,\mathrm{s}^{-1}$ of escaping ions. This number exceeds the average loss rate for the entire tail reported by *Brain et al.*, [2015] and *Dong et al.* [2015] (and is not fully accounted for in those works since the energy of the escaping ions straddles the 25 eV cutoff they utilized). This process apparently operates over a portion of the magnetospheric flank in the $-Z$ MSE hemisphere, which we estimate as having a cross-sectional area on the order of $\sim 1000 \times 3000\,\mathrm{km}^2$, based on the duration of the observations in Figures 1 and 4. If correct, this would indicate a global escape rate on the order of $3 \times 10^{23}\,\mathrm{s}^{-1}$ for this process. If continuous, this would represent an escape rate 20% that of the global total reported by *Brain et al.*, [2015], implying a significant role for bulk escape. However, a key question is "At what duty cycle does this process operate?" Future statistical studies should focus on answering this question rigorously.

Acknowledgments
We thank NASA and the Mars Exploration Program for supporting the MAVEN mission and this research. Analysis of SWEA data was partially supported by CNES. A portion of the research at NASA GSFC was supported by the NASA postdoctoral program. The MAVEN data used in this study are all archived in the Planetary Data System.

References

Brace, L. H., R. F. Theis, and W. R. Hoegy (1982), Plasma clouds above the ionopause of Venus and their implications, *Planet. Space Sci.*, *30*, 29–37.

Brain, D. A., A. H. Baker, J. Briggs, J. P. Eastwood, J. S. Halekas, and T.-D. Phan (2010), Episodic detachment of Martian crustal magnetic fields leading to bulk atmospheric plasma escape, *Geophys. Res. Lett.*, *37*, L14108, doi:10.1029/2010GL043916.

Brain, D. A., et al. (2015), The spatial distribution of planetary ion escape fluxes near Mars observed by MAVEN, *Geophys. Res. Lett.*, *42*, 9142–9148, doi:10.1002/2015GL065293.

Chapman, S. C. (1989a), Shocklike behavior exhibited at early times by the AMPTE solar wind/magnetosheath releases, *Planet. Space Sci.*, *37*, 1227–1247.

Chapman, S. C. (1989b), On the bulk motion of the ion clouds formed by the AMPTE solar wind/magnetosheath releases, *J. Geophys. Res.*, *94*, 227–240, doi:10.1029/JA094iA01p00227.

Chapman, S. C., and S. J. Schwartz (1987), One-dimensional hybrid simulations of boundary layer processes in the AMPTE solar wind lithium releases, *J. Geophys. Res.*, *92*, 11,059–11,073, doi:10.1029/JA092iA10p11059.

Connerney, J., J. Espley, P. Lawton, S. Murphy, J. Odom, R. Oliverson, and D. Sheppard (2015), The MAVEN magnetic field investigation, *Space Sci. Rev.*, doi:10.1007/s11214-015-0169-4.

DiBraccio, G. A., et al. (2015), Magnetotail dynamics at Mars: Initial MAVEN observations, *Geophys. Res. Lett.*, *42*, 8828–8837, doi:10.1002/2015GL065248.

Dong, Y., X. Fang, D. A. Brain, J. P. McFadden, J. S. Halekas, J. E. Connerney, S. Curry, Y. Harada, J. G. Luhmann, and B. M. Jakosky (2015), Strong plume fluxes at Mars observed by MAVEN: An important planetary ion escape channel, *Geophys. Res. Lett.*, *42*, 8942–8950, doi:10.1002/2015GL065346.

Dubinin, E., et al. (2008), Structure and dynamics of the solar wind/ionosphere interface on Mars: MEX-ASPERA-3 and MEX-MARSIS observations, *Geophys. Res. Lett.*, *35*, L11103, doi:10.1029/2008GL033730.

Dubinin, E., M. Fraenz, A. Fedorov, R. Lundin, N. Edberg, F. Duru, and O. Vaisberg (2011), Ion energization and escape on Mars and Venus, *Space Sci. Rev.*, *162*, 173.

Dubinin, E., M. Fraenz, J. Woch, T. L. Zhang, J. Wei, A. Fedorov, S. Barabash, and R. Lundin (2011), Bursty escape fluxes in plasma sheets of Mars and Venus, *Geophys. Res. Lett.*, *39*, L01104, doi:10.1029/2011GL049883.

Eastwood, J. P., D. A. Brain, J. S. Halekas, J. F. Drake, T. D. Phan, M. Øieroset, D. L. Mitchell, R. P. Lin, and M. Acuña (2008), Evidence for collisionless magnetic reconnection at Mars, *Geophys. Res. Lett.*, *35*, L02106, doi:10.1029/2007GL032289.

Espley, J. R., P. A. Cloutier, D. A. Brain, D. H. Crider, and M. H. Acuña (2004), Observations of low-frequency magnetic oscillations in the Martian magnetosheath, magnetic pileup region, and tail, *J. Geophys. Res.*, *109*, A07213, doi:10.1029/2003JA010193.

Fedorov, A., et al. (2006), Structure of the Martian wake, *Icarus*, *182*, doi:10.1016/j.icarus.2005.09.021.

Gunell, H., et al. (2008), Shear driven waves in the induced magnetosphere of Mars, *Plasma Phys. Controlled Fusion*, *50*, doi:10.1088/0741-3335/50/7/074018.

Gurnett, D. A., R. R. Anderson, B. Hausler, G. Haerendel, O. H. Bauer, R. A. Treumann, H. C. Koons, R. H. Holzworth, and H. Luhr (1985), Plasma waves associated with the AMPTE artificial comet, *Geophys. Res. Lett.*, *12*, 851–854, doi:10.1029/GL012i012p00851.

Gurnett, D. A., D. D. Morgan, F. Duru, F. Akalin, J. D. Winningham, R. A. Frahm, E. Dubinin, and S. Barabash (2010), Large density fluctuations in the Martian ionosphere as observed by the Mars Express radar sounder, *Icarus*, *206*, 83, doi:10.1016/j.icarus.2009.02.019.

Haerendel, G., G. Paschmann, W. Baumjohann, and C. W. Carlson (1986), Dynamics of the AMPTE artificial comet, *Nature*, *320*, 720–723.

Halekas, J. S., D. Brain, and J. P. Eastwood (2011), Large amplitude compressive "sawtooth" magnetic field oscillations in the Martian magnetosphere, *J. Geophys. Res.*, *116*, A07222, doi:10.1029/2011JA016590.

Halekas, J. S., E. R. Taylor, G. Dalton, G. Johnson, D. W. Curtis, J. P. McFadden, D. L. Mitchell, R. P. Lin, and B. M. Jakosky (2013), The Solar Wind Ion Analyzer for MAVEN, *Space Sci. Rev.*, doi:10.1007/s11214-013-0029-z.

Halekas, J. S., et al. (2015), Time-dispersed ion signatures observed in the Martian magnetosphere by MAVEN, *Geophys. Res. Lett.*, *42*, 8910–8916, doi:10.1002/2015GL064781.
Hara, T., et al. (2015), Estimation of the spatial structure of a detached magnetic flux rope at Mars based on simultaneous MAVEN plasma and magnetic field observations, *Geophys. Res. Lett.*, *42*, 8933–8941, doi:10.1002/2015GL065720.
Harada, Y., et al. (2015), Marsward and tailward ions in the near-Mars magnetotail: MAVEN observations, *Geophys. Res. Lett.*, *42*, 8925–8932, doi:10.1002/2015GL065005.
Jakosky, B. M., et al. (2015), The Mars Atmosphere and Volatile Evolution (MAVEN) mission, *Space Sci. Rev.*, doi:10.1007/s11214-015-0139-x.
Lundin, R., A. Zakharov, R. Pellinen, H. Borg, B. Hultqvist, N. Pissarenko, E. M. Dubinin, S. W. Barabasj, I. Liede, and H. Koskinen (1990), Plasma composition measurements of the Martian magnetosphere morphology, *Geophys. Res. Lett.*, *17*, 877–880, doi:10.1029/GL017i006p00877.
McFadden, J., et al. (2014), The MAVEN Suprathermal and Thermal Ion Composition (STATIC) instrument, *Space Sci. Rev.*, *195*, 199–256.
Nagy, A. F., et al. (2004), The plasma environment of Mars, *Space Sci. Rev.*, *111*, 33.
Penz, T., et al. (2004), Ion loss on Mars caused by the Kelvin-Helmholtz instability, *Planet. Space Sci.*, *52*, 1157–1167.
Rosenbauer, H., et al. (1989), Ions of Martian origin and plasma sheet in the Martian magnetosphere: Initial results of the TAUS experiment, *Nature*, *341*, 612.
Russell, C. T., J. G. Luhmann, and R. C. Elphic (1982), Magnetic field and plasma wave observations in a plasma cloud at Venus, *Geophys. Res. Lett.*, *9*, 45–48, doi:10.1029/GL009i001p00045.
Sauer, K., A. Bogdanov, and K. Baumgartel (1994), Evidence of an ion composition boundary (protonopause) in bi-ion fluid simulations of solar wind mass loading, *Geophys. Res. Lett.*, *21*, 2255–2258, doi:10.1029/94GL01691.
Szego, K., et al. (2000), Physics of mass loaded plasmas, *Space Sci. Rev.*, *94*, 429–671.
Winningham, J. D., et al. (2006), Electron oscillations in the induced Martian magnetosphere, *Icarus*, *182*, 360–370.

Erratum

In the originally published version of this article, several instances of vector signs were incorrectly typeset. The following have since been corrected and this version may be considered the authoritative version of record. In section 2. Bulk Plasma Loss Observed by MAVEN, vector signs appeared adjacent to U and B are now above (U and B represent flow velocity and magnetic field).